

Endophyte *Kwoniella mangroviensis* extract, an anti-pollution and well-aging active that preserves the microbiome and improves the lipidomic profile in the skin.

Escudero, Elizabeth¹; Perez-Aso Miguel¹; Bonini, Paolo²; Benito-Martínez, Silvia¹; Bosch, Jordi¹; **Manzano, David**^{1*}

¹PROVITAL, Barberà del Vallès, Spain; ²oloBion, Barcelona, Spain

* David Manzano, Pol. Ind. Can Salvatella - c. Gorgs Lladó, 200 - 08210 Barberà del Vallès - Barcelona (España), (+34) 93 719 23 50, d.manzano@weareprovital.com

Abstract (Maximum of 200 words)

Endophytes are symbiotic microorganisms that live inside plants promoting beneficial effects on their growth and development. They also produce bioactive compounds making them ideal candidates to identify and produce novel and sustainable cosmetic actives. In our previous study, we described the isolation of a relevant collection of plant endophytes and showed that the ferment extract of the endophyte *Kwoniella mangroviensis* (KMFE) exhibited anti-aging and anti-pollution effects *in vitro*. Now, we investigate the *in vivo* well-aging efficacy of KMFE by instrumental analysis as well as by a multi-omics study including microbiome and cutting-edge lipidome analysis of human skin volunteers. The results show that KMFE produces a clear rejuvenating effect *in vivo*, significantly improving aspects related to skin healthy appearance such as brightness, firmness, elasticity, skin relief, decreased TEWL and skin tone evenness. In addition, KMFE maintains the natural diversity of the skin's microbiome, a key factor in preventing potential alterations caused by external factors such as pollution. Finally, KMFE modulates the lipidome profile towards lipids with longer chains and decreased oxidation, thus improving the protective function of the skin barrier in polluted environments and contributes to the restructuring of a youthful and healthy skin.

Keywords: endophytes, microbiome, lipidome, ceramides, biotechnology.

Introduction

The recent years have seen an increase of knowledge regarding the human microbiome and its effects on health are now widely accepted. Although much less known, plants also possess their own symbiotic endophytic microbiome. This plant microbiota exhibits a remarkable capacity for synthesizing bioactive compounds helping plants to cope with biotic and abiotic stresses. Some of the physiological benefits that endophytes offer to plants include plant growth regulation and biological defense, as well as resistance to environmental stresses, such as drought, low temperatures, salinity, or heavy metals [1–4].

Thanks to their symbiotic relationship, these microorganisms have engineered the synthesis of secondary metabolites (SMs) including phytochemicals, which can be highly similar or even the same as those produced by their host plants. SMs mainly include alkaloids, flavonoids, terpenoids, peptides, phenols, sterols, and additional minor organic compounds [5,6]. Therefore, endophytes provide a viable alternative for producing cosmetic actives while mitigating the overexploitation of host plants. In recent years, research on plant SMs has developed rapidly, especially in the fields of human health and agricultural production [7]. Moreover, active substances with significant therapeutic effects, such as anticancer drugs, antibiotics, antiviral drugs, antidiabetic drugs, and immunosuppressive compounds, have been isolated from studied endophytes [8–11].

Due to their capacity to produce a wide range of bioactive compounds, in combination with their ability to grow under controlled conditions, endophytes are ideal candidates to develop a biomimicry-based strategy to identify novel natural sources for the sustainable development of cosmetic actives. In this context, we have successfully established a novel platform for the discovery, isolation and biotechnological production of plant endophytes as a sustainable source for natural and traceable active cosmetic ingredients.

In the framework of this platform, we have developed the first of these innovative endophyte-based ingredients, the ferment extract from the yeast *Kwoniella mangroviensis* (KMFE). We have previously reported the *in vitro* efficacy studies demonstrating the antipollution and antiaging activities of KMFE [12]. In this paper we present the results of the clinical study and further demonstrate positive antipollution and anti-aging activities of KMFE *in vivo*. To this end, we used instrumental analysis in volunteers living in a polluted city to assess the KMFE rejuvenating effect by quantifying aspects related to skin healthy appearance such as brightness, firmness, elasticity, skin relief, TEWL and skin evenness. In addition, a multi-omics study including skin microbiome and an innovative lipidome analysis of human skin volunteers was performed.

This comprehensive analysis demonstrates that KMFE is gentle on the skin and supports skin's natural microbiome, while helping to restore the shielding function of the lipid barrier in polluted environments.

Materials and Methods

Study protocol

The efficacy of KMFE was evaluated on 60 volunteers with the following characteristics:

- Age: 45 – 65 (± 2) years old with differentiated menopausal stages.
- Gender: Caucasian female living in a polluted city.
- Clinical signs of skin aging: fine lines/ wrinkles in crow's feet area and uneven complexion due to dark spots.

The duration of the study was 56 days. Instrumental parameters were evaluated at the beginning (D0), after 28 days (D28) of the treatment, and at the end (D56).

The anti-aging efficacy of the formulation was tested *in vivo* with 2 % of KMFE and compared to the efficacy of the formulation without active ingredient (placebo).

Subjects applied both products (placebo and KMFE) following the half-face method, according to a predefined randomization scheme. The formulations were applied on clean skin and on the whole face for 56 days twice a day (morning/ evening). All the evaluations were carried out under temperature and humidity-controlled conditions (temperature 18-26 °C and humidity 50 ± 10 %).

The study was carried out as follows:

- T0: Enrolment of 60 subjects according to inclusion/ non-inclusion criteria. Basal swab collection for microbiome analysis. Skin stripping for lipidomic analysis. Instrumental assessment of the parameters under study before products use (T0). Digital pictures acquisition (by means of Visia CR).
- T1-T56: daily products application (right/ left hemiface according to provided instructions).
- T28: instrumental evaluations of the parameters under study. Moreover, volunteers were asked to express their opinion on tested products by answering a questionnaire
- T56: instrumental evaluations of the parameters under study; digital pictures acquisition (by means of Visia CR); swab collection for microbiome analysis; skin stripping for lipidomic analysis. Moreover, volunteers were asked to express their opinion on tested products by answering a questionnaire.

For those volunteers with postmenopausal condition, the panel was divided in a subgroup (n=17) and some key instrumental parameters related to this condition were analyzed.

Instrumental measurements

Skin gloss

The gloss parameter was analyzed by using the spectrophotometer/ colorimeter CM-700D (Konica-Minolta). All measures were taken on the cheek area. Means and standard deviations were calculated.

Skin elasticity

Skin elasticity and firmness evaluation were performed using a Cutometer® dual MPA 580 (Courage & Khazaka, Germany) with a 2 mm probe. The cutometer measures the deformation of the skin. In this study, the following parameters were analyzed: R0 (skin distensibility or firmness), R2 (gross-elasticity), and R9 (tiring effects of the skin). The measurement area was on the cheek of each subject. Means and standard deviations were calculated.

Transepidermal Water Loss (TEWL)

Transepidermal water loss is measured using a Tewameter® TM 300 (Courage+Khazaka, electronic GmbH). The following equation which represents the Diffusion law (discovered by Adolf Fick in 1855) is the basis for the measurement:

$$\frac{dm}{dt} = -D \times A \times \frac{dp}{dx}$$

where:

A = surface in m²; water transported (in g); time (h); diffusion constant (=0.0877 g/mhmm Hg); atmosphere vapor pressure (mm Hg); distance from skin surface to point of measurement (m).

The measurement area was on each subject's cheek. Means and standard deviations were calculated.

Skin profilometry

Skin surface is quantitatively assessed by Primos 3D (GFMesstechnik GmbH). In this study the following parameters were evaluated in the crow's feet area: Skin isotropy, Ra (skin smoothness) and RZ (roughness).

Skin complexion evenness

The skin complexion evenness is measured by a colorimetric image analysis technique (Visia®-CR, Canfield Scientific). The measured parameter is the variance of color distribution of the

cross-filter images. The standard deviation of the histogram of color distribution inside the region of interest is measured using a dedicated image analysis software.

Self-assessment

After 28 and 56 days of product use, the sixty volunteers were asked to express their opinion on tested products (performance and pleasantness) by answering to a questionnaire which gathers the items concerning the efficacy of the product:

- My skin is firmer.
- The product helps to improve the appearance of my skin.
- The skin texture is visibly improved.
- The signs of aging are reduced.
- My skin complexion is more uniform.

For each question, the subjects answered according to a defined grading scale and the results were expressed in percentage of people answered each question.

Statistical data treatment

For each parameter and time point of analysis, the absolute values obtained during the study were used to calculate the variation vs D0 and the % of variation vs D0 (% var vs D0). The means and standard deviations of the % var values were then calculated and represented. Normal distribution of data was evaluated using the Shapiro–Wilk W-test. Differences between results obtained by groups applying KMFE and placebo were analyzed by the t-student test for normal distributions, and by Wilcoxon Signed Rank test or Mann-Whitney test for non-normal distributions. All the calculations were performed using GraphPad Prism® v8 software. A 95% level of significance was adopted.

Skin microbiome: Study design

The skin microbiome analysis is based on metagenomic analysis of the 16S rRNA gene. 16S rRNA gene was chosen since this gene is present in all bacterial (prokaryotic) cells genetic material, but not in human (eukaryotic) cells. Skin microbiota was collected at T0 and T56 by brushing a defined skin area for each half-face with a swab, a non-invasive method allowing to collect the bacteria on the skin surface. The second step of the analysis pipeline consisted of isolating the bacterial DNA from other components of the sample. The bacterial material in each sample was amplified by PCR to first, increase the quantity of DNA, and second, to label the genetic material in each sample. Samples' concentrations were levelled out prior to pooling, to obtain the sequencing mix. This solution was loaded in a cartridge and analyzed by a sequencer. At the end of the metagenomic analysis run, the raw files were analyzed, and the Shannon and Simpson Alpha diversity indexes were calculated with the phyloseq R package [13].

Skin lipidome: Study design

Samples from the first layers of the stratum corneum were collected from the cleaned skin of the cheeks by means of tape stripping procedure using Corneofix® (Courage+Khazaka, electronic GmbH). Five consecutive tape strips were collected from the same skin area. The first four stripped layers were discarded, and strip n. 5 was collected and stored at -80 °C for further analysis. Each sample was extracted following procedure described by Sadowski et al. [14].

The extracted samples were analyzed using Agilent Technologies (Santa Clara, California, CA, USA) 1290 Infinity II liquid chromatograph UHPLC coupled to a 6560 Ion Mobility Q-TOF detector. An identification of all kinds of lipidic molecules was obtained (peak intensity).

For quality control, validation and retention time locking 69 deuterated standards from 14 lipids classes spiked into all samples were aligned, corrected, and used for signal intensity calibration and validation. Compound identification was achieved by four-dimensional data 4D-ID® using a custom version of the lipidome atlas, MSDIAL 4. Differential analysis and enrichment analysis,

including lipid chain length analysis, were performed with lipidr package [15] on R version 4.2.1. [16]. The most abundant lipids were used to predict the oxidation with LPPTiger2 [17].

Results

Skin radiance and transepidermal water loss (TEWL)

To evaluate the effect of KMFE on gloss improvement, a comparison between KMFE and placebo was made after 28 and 56 days of treatment. The main results for the % var of Gloss parameter are summarized in Figure 1 A. It is shown that the treatment with KMFE exerted a 12.54 % and 16.66 % statistically significant increase after 28 and 56 days, respectively, compared to the placebo treatment.

On the other hand, trans-epidermal water loss (TEWL) is the most widely used objective measurement for assessing the barrier function of skin. TEWL is the quantity of condensed water that diffuses across a fixed area of stratum corneum to the skin surface per unit time.

As it can be observed in the results presented in Figure 1 B, KMFE decreased this parameter by -1.7 % and -3.87 % after 28 and 56 days of treatment, respectively. The difference between both treatments is statistically significant after 28 and 56 days of product application.

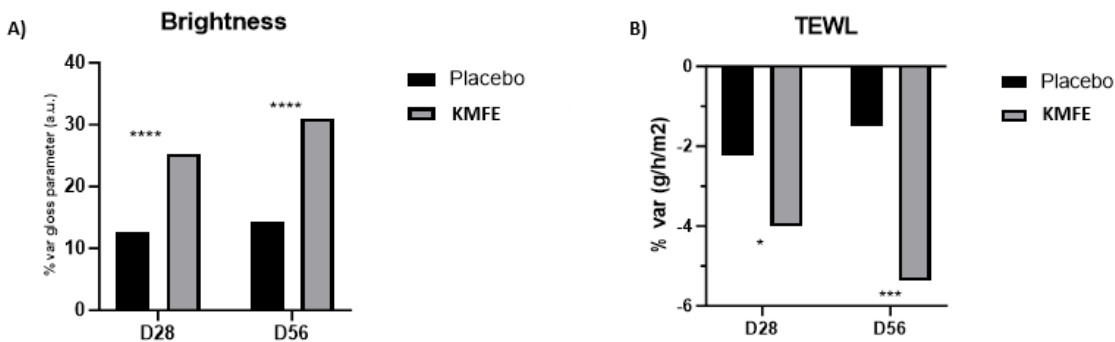


Figure 1. A) Skin gloss variation (% of change) during the study. Mean values of all the subjects (n=60 for each treatment). Statistical comparison between both treatments (****p <0,0001). **B)** Skin TEWL variation (% of change) during the study. Mean values of all the subjects (n=60 for each treatment). Also shown the statistical comparison between both treatments (*p<0.05 at 28 days and ***p<0.001 at 56 days).

Skin firmness and elasticity

Results from R0, R2 and R9 parameters are summarized in Figure 2. The treatment with KMFE showed a significant -7.56 % decrease in the % var of **R0** parameter (top graph) when compared to placebo after 56 days of use. This result confirms the action of KMFE directly on the collagen fibers, responsible for skin resistance, firmness, thickness, and tightness.

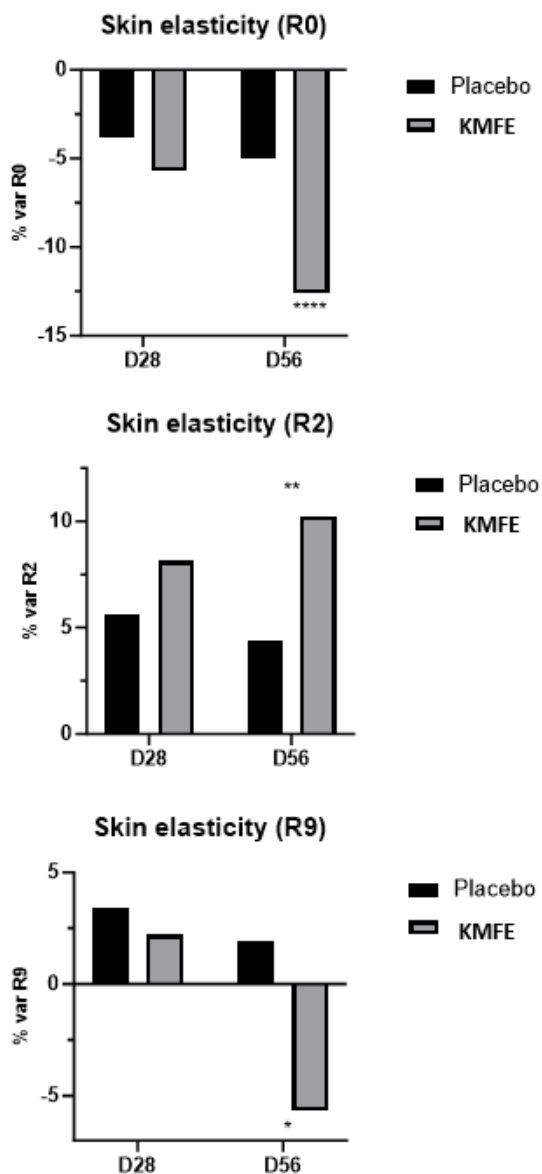


Figure 2. Skin elasticity variation in R0, R2 and R9 parameter (% of change) during the study. Mean values of all the subjects (n=60 for each treatment). Also shown the statistical comparison between both treatments (*p<0.05 at 56 days, **p<0.01 at 56 days, ****p<0.0001 at 56 days).

The **R2** parameter measures the ability of the skin to return to its original position after stressing event or deformation and is related to skin elastic fibers' function. As it is shown in Figure 2 (middle graph), KMFE was able to significantly increase this parameter at day 56 by a 5.81 % (% of var) compared to the placebo treatment.

Finally, **R9** parameter is correlated with skin fatigue. Repeated suction and release with Cutometer provoke skin fatigue, resulting in decreased elasticity and increased maintenance of the deformed position. Dobrev [18] reported that adult skin shows a higher degree of fatigue than young skin. As shown in Figure 2 (bottom graph), treatment with KMFE improved this parameter at day 56 compared to the treatment with placebo (% of var). The decrease of the R9 parameter in relation to placebo was statistically significant by -7.54 % at D56.

Skin profilometry

Results obtained for isotropy, Ra and Rz (% var) are shown in Figure 3. First, it was found that isotropy (top graph) had increased after 28 and 56 days of treatment when KMFE is compared to placebo treatment. This percentage of change (4.3 %) was statistically significant at day 56.

The same effect was observed when analyzing Ra parameter (middle graph) at day 28 and day 56 of treatment with KMFE, where a decrease down to -3.78 % at day 28 and -5.46 % at day 56 was measured in comparison with placebo. This percentage of change was statistically significant at day 28 and day 56.

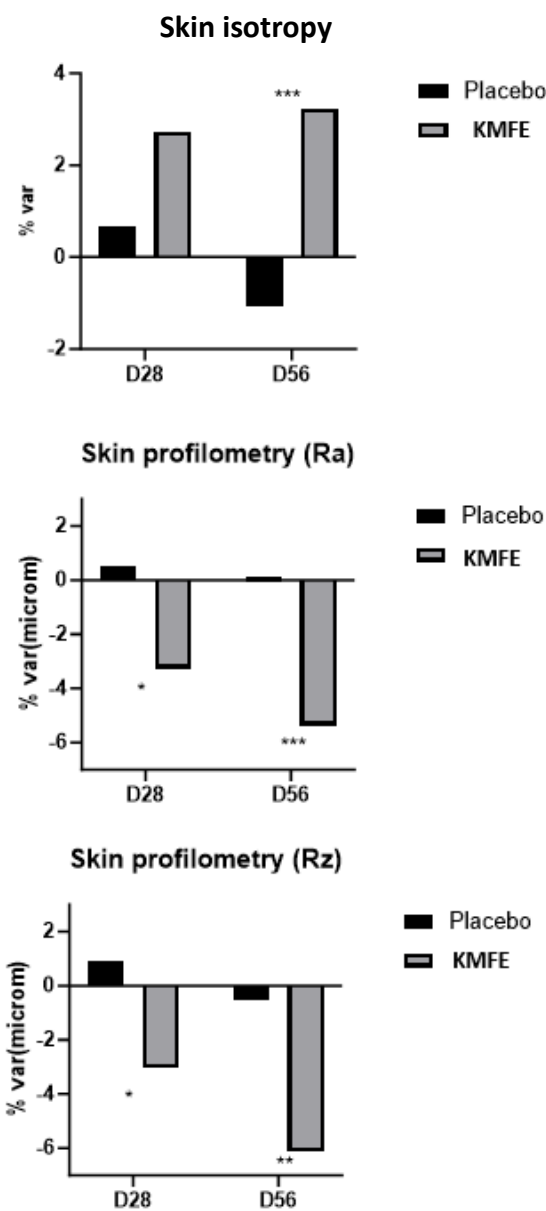


Figure 3. Isotropy, Ra and Rz parameters evolution (% change) during the study. Mean values of all the subjects (n=60 for each treatment). Also shown the statistical comparison between both treatments (*p<0.05 at day 28, **p<0.01 at 56 days and ***p<0.001 at 56 days).

Finally, Rz parameter (bottom graph) was also measured. The facial treatment with KMFE determined a statistically significant increase of this parameter (% var) at each experimental monitored time. Results obtained with the use of facial treatment with KMFE showed a decreased of -3.95 % and -5.56 % in Rz at day 28 and day 56, respectively compared to placebo.

Skin evenness

The facial treatment with KMFE determined a statistically significant improvement of skin evenness (skin tone color variation) at day 56. A decrease of standard deviation value of color distribution indicates an improvement of skin complexion evenness. Results obtained with the use of KMFE facial treatment showed a decrease of -2.7% and -4.48% in this parameter at day 28 and day 56, respectively, compared to placebo treatment (Figure 4). Thus, indicating a clear improvement in the skin evenness.

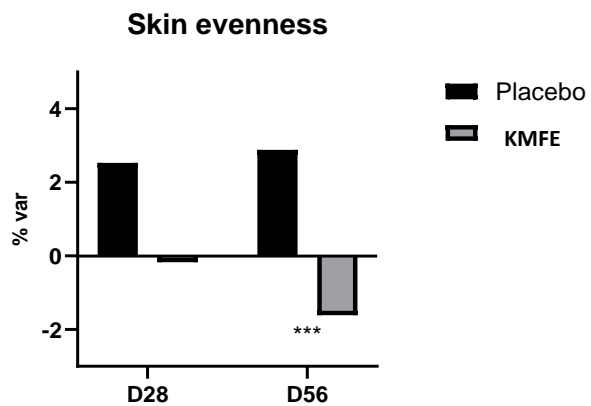


Figure 4. Skin evenness evolution (% of change) during the study. Mean values of all the subjects (n=60 for each treatment). Also shown the statistical comparison between both treatments (***(p<0.001 at 56 days).

Since aged skin shows uneven complexion, KMFE has revealed its properties to reverse these aging uneven signs.

Pictures of the skin of volunteers were acquired by means of Visia®-CR (Canfield Scientific). Representative images of the skin improvement after treatment with KMFE are presented in Figure 5 below.



Figure 5. VISIA cross-polarized images: A) Hemiface view of a volunteer treated with KMFE at T0 and T56; B) hemiface view of the same volunteer treated with placebo at T0 and T56.

As it can be observed, a clear improvement in the evenness was evident after the treatment with KMFE. Mainly, skin redness and spots were improved leading to a more uniform complexion.

***In vivo* efficacy results in the post-menopausal panel**

Data from 17 volunteers with age ranging from 54 to 67 years with post-menopause condition were separated from the whole panel and analyzed as a sub-group. The results of the mentioned instrumental tests were evaluated at D0, D28 and D56.

Interestingly, the postmenopausal sub-group showed even a greater improvement for certain key parameters (Table I), including TEWL, directly linked to barrier function, brightness which showed a significantly stronger increase, and further improvement on the skin tone uniformity and profilometry.

	D28	D56	
	Total	Total	Post-Menopausal
TEWL	-1.7%*	-3.9%***	-5.2%**
Brightness	+12.5%****	+16.6%****	+21.0%****
Color variation	-2.7%*	-4.5%***	-6.6%**
Microstructure	2.05	+4.3%***	+5.3%*

Table I. Comparative summary table with the results of the instrumental analysis of TEWL, brightness, color variation and microstructure at days 28 and 56 of the full panel and at day 56 of the postmenopausal sub-group.

Self-assessment of the product efficacy

The self-assessment included a subjective evaluation of 5 aspects regarding efficacy of KMFE and placebo treatments, (data not shown). Quantification of positive answers showed that KMFE was superiorly evaluated in comparison with placebo, being statistically significant the items related to “skin texture improvement” and “signs of aging reduced” (youthfulness).

Microbiome analysis results

For this study, the skin of volunteers from urban areas was treated with either KMFE or Placebo for 56 days. Then, samples were taken at D0 and D56 and analyzed by 16S sequencing. Interestingly, the skin microbiota diversity, measured by two different indexes, Shannon, and Simpson (Figure 6), was not altered during the 56-day period by neither Placebo nor KMFE, indicating that KMFE is gentle on the skin and supports skin's natural microbiome.

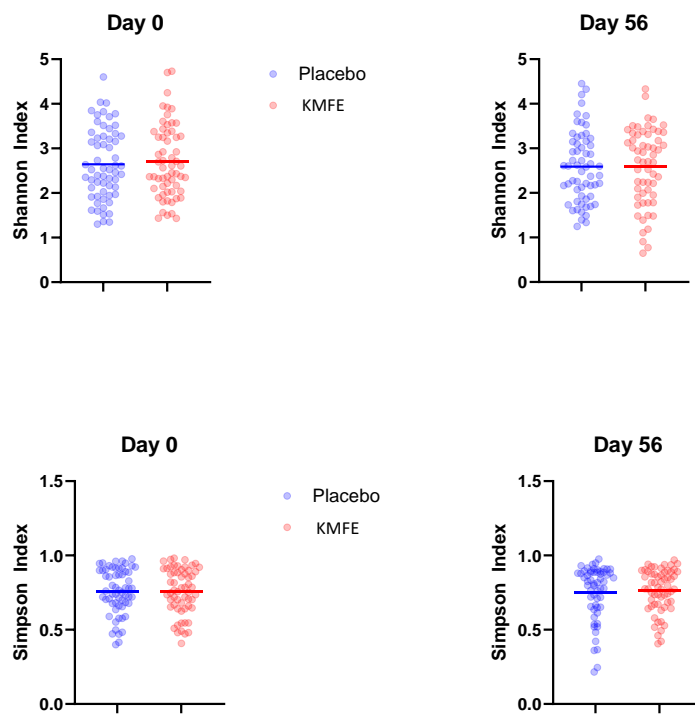


Figure 6. Skin microbiota diversity measured by two different indexes, Shannon and Simpson.

Lipidome analysis results

We analyzed 240 stratum corneum samples from 60 volunteers treated with KMFE or Placebo, in hemiface at two time points (D0 and D56) and identified 327 different lipids in the collected samples. Specifically, these 327 different lipid species corresponded to 5 major lipid categories, which were found in the following proportion: 78.90 % Glycerolipids [GL], 15.60 % Sphingolipids [SP], 3.36 % Fatty Acyls [FA], 1.53 % Glycerophospholipids [GP] and 0.61 % Sterol Lipids [ST] (data not shown). These categories are further subdivided into Main Lipid Classes, of which the ratio of our *in vivo* study results is represented in Figure 7, with the following Lipid Classes at their highest proportion: 54.13 % Triacylglycerols [GL03], 19.27 % Diacylglycerols [GL02] and 13.76 % Ceramides [SP02].

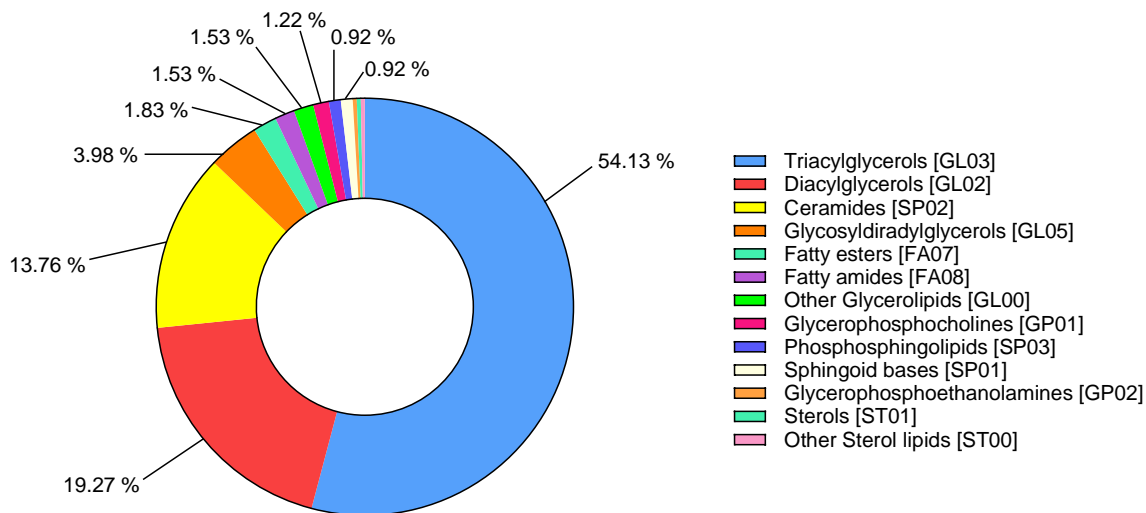


Figure 7. Percentage representation of the Main Lipid Classes to which the 327 lipids identified in the study correspond to. Lipid molecules belong to 5 different major Lipid Categories, which are divided into 14 Lipid Main Classes and 24 Lipid Classes.

Interestingly, 114 lipids were found significantly different when comparing the application of KMFE versus Placebo at day 56. To better understand the effect of KMFE on these lipids, further bioinformatics analysis was performed.

Lipidomic study: enrichment analysis

We performed a bioinformatic analysis with the differentially regulated lipids to understand the impact of KMFE during the 56-day period of product application on the skin lipidome. The enrichment analysis, where different lipid properties are assessed, (i.e. lipid class, chain length and unsaturation), considering not only lipids individually but the whole lipidome, revealed that KMFE changed the lipid profile of the skin by mainly increasing the quantity of long chain lipids.

In this regard, in Figure 8 A below, we can appreciate that the application of KMFE for 56 days increased the total chain length trend of the whole lipidome by increasing the amount of lipids with long chains (A; top graph). Remarkably, this was not the case for application of Placebo for 56 days (A; bottom graph):

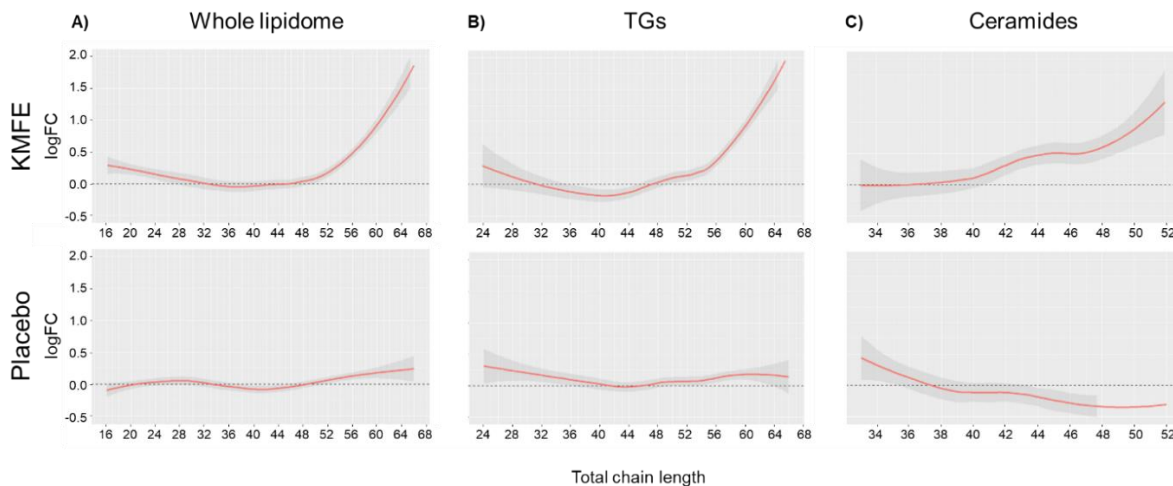


Figure 8. Trend analysis of the lipids chain length after application of KMFE (top graphs) and placebo (bottom graphs) for 56 days. A) Total chain length trend of the whole lipidome. B) Trend analysis of the length of the Triglycerides (TGs). C) Trend analysis of the length of the Ceramides.

Upon further assessment, we found that this change on the lipidome profile, was partially due to an increase in the length of the chains of Triglycerides (TGs). In this regard, we detected 55 different TGs that were significantly regulated by KMFE. A trend analysis of the length of the TGs chains revealed that KMFE increased TGs with very long total chain length, as depicted in Figure 8 B (top graph). Again, this was not the case for Placebo (B; bottom graph).

Interestingly, KMFE also presented strong differences to placebo when analyzing its influence on the chain length of ceramides. As depicted in Figure 8 C, KMFE increases the length of ceramide chains during the 56-day period (C; top graph). While placebo slightly decreased the ceramides with long chain lengths during the same period (C; bottom graph).

Of note, when comparing ceramides of volunteers stimulated with KMFE to those stimulated with placebo, 31 ceramides were found significantly modified, among which 29 were increased and 2 decreased. Those increased ceramides were long carbon chain ceramides, including an increase by 34.51 % of the long chain Ceramide NS, one of the most abundant in human skin in the facial area [19].

Oxidized lipid study

To continue with the lipidome analysis, a second bioinformatic evaluation focused on the peroxidation level of skin lipids from the same panel of volunteers. The analytical assessment revealed that KMFE outperforms Placebo in reducing lipid oxidation (Table II). This effect is notably pronounced for specific triglycerides (TGs), which exhibit a decreased oxidation rate being statistically significant for some particular species where we could find a reduction in oxidation rate of up to -32 %** ($p<0.01$).

Furthermore, KMFE treatment revealed a significant decrease of hydroperoxy-squalene (Sq-OOH) down to 24 %* ($p<0.05$). Oppositely, placebo demonstrated a limited protective effect in only three lipids, failing to reach statistical significance on others.

Alignment ID	Lipid name	p (Welch)	fc
54937	TG(18:1_18:1_9:0<oxo>)#[M+Na]+	1.30028E-10	0.25
60505	TG(18:1_18:2_12:1<OH,oxo>)#[M+Na]+	0.001687531	0.41
60258	TG(18:1_18:2_12:1<2oxo>)#[M+Na]+	0.00789409	0.68
15336	3-Hydroperoxy-squalene C4	0.026478009	0.76
68088	TG(18:1_18:1_18:2<OH,oxo>)#[M+Na]+	0.037398352	0.54
65864	TG(16:0_18:1_18:2<OH,oxo>)#[M+Na]+	0.054271911	0.64

Alignment ID	Lipid name	p (Welch)	fc
54937	TG(18:1_18:1_9:0<oxo>)#[M+Na]+	3.2511E-05	0.48
60505	TG(18:1_18:2_12:1<OH,oxo>)#[M+Na]+	0.000999163	0.42
68088	TG(18:1_18:1_18:2<OH,oxo>)#[M+Na]+	0.047070676	0.54

Table II. Statistical evaluation of the effect of KMFE (top chart) and placebo (bottom chart) on the amount of oxidized lipids. Data show fold-change variation comparing D56 vs D0.

Discussion

Skin epidermal barrier protects the body from surrounding environmental aggressions including pollution. There are several mechanisms through which air pollutants cause skin damage and aging, i.e., increased oxidative stress, promotion of a pro-inflammatory environment in the skin and barrier disruption, and alteration of the skin microbiome [20]. In this context, our previous *in*

vitro study [12] provided evidence for antipollution as well as anti-aging activities of a ferment extract from the endophyte *Kwoniella mangroviensis* (KMFE).

Our *in vitro* studies revealed that KMFE exhibited antipollution effects by means of reducing ROS and inflammatory mediators as demonstrated in human keratinocytes exposed to urban dust. Besides, by RNA-Seq whole-transcriptome analysis, we revealed the capacity of KMFE to induce the formation of extracellular matrix (ECM) in human dermal fibroblasts (HDF), indicating a significant anti-aging activity. Furthermore, at the protein level, collagen I and elastin content significantly increased by KMFE in HDF. Thus, our previous *in vitro* work strongly proved that KMFE elicits a protection against the deleterious effects caused by pollution and has an antiaging activity at both the gene and protein levels.

Interestingly, in the present study we show that KMFE produces a clear rejuvenating effect *in vivo*, significantly improving aspects related to skin healthy appearance such as brightness, firmness, elasticity, skin relief, decreased TEWL and skin evenness. In this regard, firmness and elasticity are viscoelastic parameters that vary throughout the aging process or due to skin pathologies. In relation to aging, the elastic properties of the skin are essential for wrinkle prevention and here we show that KMFE improves the elastic properties of the skin. On the other hand, normal skin aging is characterized by an alteration of the underlying connective tissue with measurable consequences on global skin biophysical properties, and skin relief highly changes. In fact, the cutaneous lines change from a relative isotropic orientation to a high anisotropic orientation [21]. Our results reveal that KMFE can counteract the deleterious effects of aging by significantly increasing the isotropic orientation and improve the smoothness parameters Ra and Rz. The reorganization of the skin relief during the aging process might be due to a modification of skin mechanical properties, particularly, a modification within the dermis. Accordingly, we demonstrated the *in vitro* capacity of KMFE to induce ECM remodeling.

In addition, postmenopausal skins had a superior improvement at parameters like color evenness, TWEL, brightness and skin isotropy, when compared to the global panel, suggesting a better performance of KMFE in such mature skins, making it the perfect solution to combat skin aging signs.

On the other hand, the skin microbiome is an integral part of the skin barrier that can affect its health by modulating host immune responses and barrier function [22]. Dysbiosis of the microbiome has been associated with various diseases. There is increasing evidence indicating a link between undesirable skin conditions with altered microbial assembly process and a more fragile microbiome network [23], [24]. Specifically, a cooccurrence network of the microbiome was found to be affected by environmental factors [25]. In a study of the skin microbiome in China, a more fragile microbial network was found in urbanized environments where higher incidence of skin diseases has been observed [23]. Skin microbiome, the first layer of the skin barrier [26], could mediate the effect of urban living on skin physiology. In this respect, our study has proven that KMFE preserves the diversity of the skin's natural microbiome of volunteers living in a polluted environment.

Regarding our cutting-edge lipidomic study, the aim was to elucidate if KMFE helps to improve the skin barrier and protects lipids from oxidation. The skin is a complex and highly specialized organ serving multiple functions in the body, the principal of which is to provide a barrier that prevents water loss and protects the body from adverse environmental agents [27]. This function is mediated mainly by the stratum corneum (SC)—the outermost layer of the epidermis, consisting of dead flattened keratinocytes embedded in a lipid matrix, acting together as a “brick and mortar” system difficult to penetrate [28]. The lipids that constitute the extracellular lamellar matrix of the SC have a unique composition and exhibit distinctive properties. The major lipids of the human SC are ceramides, cholesterol, and fatty acids (FAs), comprising approximately 50 %, 25 % and 15 % of the total lipid mass, respectively. FAs have multiple roles in the epidermis,

and they are found as free FAs (FFAs) and in bound form in neutral lipids, mainly triglycerides (TGs) [29].

Interestingly, it is well described that long-chain lipids are an important component for skin's barrier function [30]. In fact, the enzymes responsible for the elongation of very long fatty acids (ELOVL 1 and ELOVL4) are needed for a proper production of long FAs to develop competent cutaneous permeability barrier [31–33]. Besides, in diseases where lipid chain length is reduced, a decrease in the barrier's performance is observed due to an alteration on the packing of lipids [34]. Similarly, reduction in lipid chain length is correlated with less dense lipid organization and a decreased skin barrier function in conditions such as atopic eczema [35]. In this sense, this study has demonstrated that KMFE increases the content of long chain lipids and protects from oxidative damage, strongly suggesting that KMFE modulates the lipidome profile towards a stronger "mortar", improving lipid packing and organization, contributing to a better barrier function of the skin in polluted environments. Interestingly, these results are in completely agreement with the reduction of TEWL observed on the skin of the volunteers treated with KMFE (figure 1B and Table I).

Moreover, mitigating lipid peroxidation prevents degradation of cellular membrane's structure function, delaying skin aging and the exacerbation of dermatological disorders [29]. In particular, we show a significant decrease of Sq-OOH, a molecule involved in UV-induced epidermal cell changes and skin disorders. Sq-OOH, when applied topically, has been shown to induce wrinkle formation, and other signs of skin damage and aging, including changes in skin roughness, decreased skin conductance, hyperkeratosis, and epidermal thickening [36]. Our findings suggest that KMFE confers a protective effect against oxidative stress.

Of particular interest are ceramides, since their chain length is also essential for a correct barrier function, directly correlated with a decrease in TEWL [37]. Thus, short-chain ceramides do not maintain barrier properties as long-chain ceramides [38]. Among the different ceramides

identified, we found KMFE differentially regulated the long ceramide NS (Cer[NS]; also named ceramide II), one of the most abundant ceramides in the SC (21% of total SC ceramides) [19], with chain length >40 total carbons. Importantly, KMFE increased endogenously Cer[NS] by up to 34.51 % *in vivo*. It has been reported that the amount of Cer[NS] with 34 total carbons (short Cer[NS]) is strongly correlated with the impaired SC functions (higher TEWL and lower capacitance) [39]. In this sense, a recent study [40] has shown that menopause reduces the average chain length of SC ceramides. In addition to their abundance, quality of ceramides is also important to the SC structure, with shorter ceramides leading to impaired barrier function as explained before. Total average carbon number of ceramides was lower in post-menopausal women, with significant reduction in the total carbon number of the Cer[NS], among others [40]. Also, it was found that ceramide length, but not abundance, negatively correlates with TEWL allowing more water loss in post-menopause skin [40]. Accordingly, our *in vivo* efficacy study shows that in the post-menopausal volunteers (54-67 years old) parameters such as TEWL, gloss, evenness and isotropy showed a remarkable improvement of -5.21%, 21%, -6.6% and +5.3% (% of var), respectively, when compared to placebo after 56 days.

Our study proves that the barrier function and permeability of the SC is strengthened after KMFE application by decreasing TEWL, improving skin texture and increasing skin gloss, as well as enhancing color evenness in all volunteers and specially in post-menopause volunteers.

Conclusion

We have developed a biotechnology platform to identify and produce active cosmetic ingredients derived from plant endophytes. We have isolated a relevant collection of endophytic strains and screened for bioactivities to select the best candidates for subsequent developments.

The results presented in this study reveal that KMFE has the capacity to induce a visible anti-aging effect *in vivo* leading to a more luminous and elastic skin, as well as improving the TEWL, the profilometry, and evenness of the skin, providing a solution to combat skin aging. Also, KMFE

is gentle with skin's natural microbiome, preserving its ecological diversity. Finally, KMFE reduces lipid oxidation and modulates the lipidome profile towards lipids with longer length chains. These insightful results imply that this innovative ingredient improves the packing and organization of lipids, thus strengthening the barrier function from within and providing an integral protection to skins in polluted environments.

Conflict of Interest Statement

NONE.

References

1. Jin Z, Gao L, Zhang L, Liu T, Yu F, Zhang Z, et al. Antimicrobial activity of saponins produced by two novel endophytic fungi from *Panax notoginseng*. *Nat Prod Res*. 2017;31.
2. Wei G, Dong L, Yang J, Zhang L, Xu J, Yang F, et al. Integrated metabolomic and transcriptomic analyses revealed the distribution of saponins in *Panax notoginseng*. *Acta Pharm Sin B*. 2018;8.
3. Xie J, Wu YY, Zhang TY, Zhang MY, Peng F, Lin B, et al. New antimicrobial compounds produced by endophytic *Penicillium janthinellum* isolated from *Panax notoginseng* as potential inhibitors of FtsZ. *Fitoterapia*. 2018;131.
4. Xie J, Wu YY, Zhang TY, Zhang MY, Zhu WW, Gullen EA, et al. New and bioactive natural products from an endophyte of: *Panax notoginseng*. *RSC Adv*. 2017;7.
5. Kubala S, Garnczarska M, Wojtyla Ł, Clippe A, Kosmala A, Zmieleńko A, et al. Deciphering priming-induced improvement of rapeseed (*Brassica napus* L.) germination through an integrated transcriptomic and proteomic approach. *Plant Science*. 2015;231.
6. Tian N, Liu F, Wang P, Zhang X, Li X, Wu G. The molecular basis of glandular trichome development and secondary metabolism in plants. *Plant Gene*. 2017.
7. Bitchagno GTM, El Bouhssini M, Mahdi I, Ward JL, Sobeh M. Toward the Allelopathy of *Peganum* sp. and Related Chemical Constituents in Agriculture. *Front Plant Sci*. 2022.
8. Gouda S, Das G, Sen SK, Shin HS, Patra JK. Endophytes: A treasure house of bioactive compounds of medicinal importance. *Front Microbiol*. 2016.
9. Debbab A, Aly AH, Proksch P. Bioactive secondary metabolites from endophytes and associated marine derived fungi. *Fungal Divers*. 2011.
10. Rai N, Kumari Keshri P, Verma A, Kamble SC, Mishra P, Barik S, et al. Plant associated fungal endophytes as a source of natural bioactive compounds. *Mycology*. 2021.

11. Preethi K, Mani VM, Lavanya N. Endophytic Fungi: A Potential Source of Bioactive Compounds for Commercial and Therapeutic Applications. *Endophytes: Potential Source of Compounds of Commercial and Therapeutic Applications*. 2021.
12. Manzano D, Perez-Aso M, Escudero E, Akalin A, Vatsellas G, De Vos RCH, et al. A novel platform for the discovery and biotechnological production of plant endophytes as a source for cosmetic actives. IFSCC; 2023.
13. McMurdie PJ, Holmes S. Phyloseq: An R Package for Reproducible Interactive Analysis and Graphics of Microbiome Census Data. *PLoS One*. 2013;8.
14. Sadowski T, Klose C, Gerl MJ, Wójcik-Maciejewicz A, Herzog R, Simons K, et al. Large-scale human skin lipidomics by quantitative, high-throughput shotgun mass spectrometry. *Sci Rep*. 2017;7.
15. Mohamed A, Molendijk J, Hill MM. Lipidr: a software tool for data mining and analysis of lipidomics datasets. *J Proteome Res*. 2020;19:2890–7.
16. R Development Core Team. R: A language and environment for statistical computing. Vienna, Austria. www.R-project.org. 2018.
17. Ni Z, Angelidou G, Hoffmann R, Fedorova M. LPPtiger software for lipidome-specific prediction and identification of oxidized phospholipids from LC-MS datasets. *Sci Rep*. 2017;7.
18. Dobrev H. Application of Cutometer area parameters for the study of human skin fatigue. *Skin Research and Technology*. 2005;11.
19. Coderch L, Lopez O, de la Maza A, Parra JL. Ceramides and Skin Function. *Am J Clin Dermatol*. 2003;4:107–29.
20. Mancebo SE, Wang SQ. Recognizing the impact of ambient air pollution on skin health. *Journal of the European Academy of Dermatology and Venereology*. 2015.
21. Pailler-Mattei C, Debret R, Vargiolu R, Sommer P, Zahouani H. In vivo skin biophysical behaviour and surface topography as a function of ageing. *J Mech Behav Biomed Mater*. 2013;28.
22. Wang L, Xu Y-N, Chu C-C, Jing Z, Chen Y, Zhang J, et al. Facial Skin Microbiota-Mediated Host Response to Pollution Stress Revealed by Microbiome Networks of Individual. *mSystems*. 2021;6.
23. Kim HJ, Kim H, Kim JJ, Myeong NR, Kim T, Park T, et al. Fragile skin microbiomes in megacities are assembled by a predominantly niche-based process. *Sci Adv*. 2018;4.
24. Strona G, Lafferty KD. Environmental change makes robust ecological networks fragile. *Nat Commun*. 2016;7.
25. Röttgers L, Faust K. From hairballs to hypotheses—biological insights from microbial networks. *FEMS Microbiol Rev*. 2018.
26. Grice EA, Segre JA. The skin microbiome. *Nat Rev Microbiol*. 2011;9:244–53.
27. Proksch E, Brandner JM, Jensen JM. The skin: An indispensable barrier. *Exp Dermatol*. 2008;17.

28. Khnykin D, Miner JH, Jahnsen F. Role of fatty acid transporters in epidermis: Implications for health and disease. *Dermatoendocrinol.* 2011.
29. Feingold KR. The role of epidermal lipids in cutaneous permeability barrier homeostasis. *J Lipid Res.* 2007.
30. Flori E, Mastrofrancesco A, Ottaviani M, Maiellaro M, Zouboulis CC, Camera E. Desaturation of sebaceous-type saturated fatty acids through the SCD1 and the FADS2 pathways impacts lipid neosynthesis and inflammatory response in sebocytes in culture. *Exp Dermatol.* 2023;32.
31. Tawada C, Kanoh H, Nakamura M, Mizutani Y, Fujisawa T, Banno Y, et al. Interferon- γ decreases ceramides with long-chain fatty acids: Possible involvement in atopic dermatitis and psoriasis. *Journal of Investigative Dermatology.* 2014;134.
32. Li W, Sandhoff R, Kono M, Zerfas P, Hoffmann V, Ding BCH, et al. Depletion of ceramides with very long chain fatty acids causes defective skin permeability barrier function, and neonatal lethality in ELOVL4 deficient mice. *Int J Biol Sci.* 2007;3.
33. Cameron DJ, Tong Z, Yang Z, Kaminoh J, Kamiyah S, Chen H, et al. Essential role of Elovl4 in very long chain fatty acid synthesis, skin permeability barrier function, and neonatal survival. *Int J Biol Sci.* 2007;3.
34. Vasireddy V, Uchida Y, Salem N, Kim SY, Mandal MNA, Reddy GB, et al. Loss of functional ELOVL4 depletes very long-chain fatty acids (\geq C28) and the unique ω -O-acylceramides in skin leading to neonatal death. *Hum Mol Genet.* 2007;16.
35. van Smeden J, Janssens M, Kaye ECJ, Caspers PJ, Lavrijzen AP, Vreeken RJ, et al. The importance of free fatty acid chain length for the skin barrier function in atopic eczema patients. *Exp Dermatol.* 2014;23.
36. Chiba K, Sone T, Kawakami K, Onoue M. Skin roughness and wrinkle formation induced by repeated application of squalene-monohydroperoxide to the hairless mouse. *Exp Dermatol.* 1999;8.
37. Janssens M, Van Smeden J, Gooris GS, Bras W, Portale G, Caspers PJ, et al. Increase in short-chain ceramides correlates with an altered lipid organization and decreased barrier function in atopic eczema patients. *J Lipid Res.* 2012;53.
38. Školová B, Januiššová B, Zbytovská J, Gooris G, Bouwstra J, Slepčka P, et al. Ceramides in the skin lipid membranes: Length matters. *Langmuir.* 2013;29.
39. Ito S, Ishikawa J, Naoe A, Yoshida H, Hachiya A, Fujimura T, et al. Ceramide synthase 4 is highly expressed in involved skin of patients with atopic dermatitis. *Journal of the European Academy of Dermatology and Venereology.* 2017;31.
40. Kendall AC, Pilkington SM, Wray JR, Newton VL, Griffiths CEM, Bell M, et al. Menopause induces changes to the stratum corneum ceramide profile, which are prevented by hormone replacement therapy. *Sci Rep.* 2022;12.